

Driving Potency with Rotationally Stable Atropisomers: Discovery of Pyridopyrimidinedione-Carbazole Inhibitors of BTK

Anurag S. Srivastava,* Soo Ko, Scott H. Watterson,* Mark A. Pattoli, Stacey Skala, Lihong Cheng, Mary T. Obermeier, Rodney Vickery, Lorell N. Discenza, Celia J. D'Arienzo, Kathleen M. Gillooly, Tracy L. Taylor, Claudine Pulicchio, Kim W. McIntyre, Shiuhan Yip, Peng Li, Dawn Sun, Dauh-Rung Wu, Jun Dai, Chunlei Wang, Yingru Zhang, Bei Wang, Joseph Pawluczyk, James Kempson, Rulin Zhao, Xiaoping Hou, Richard Rampulla, Arvind Mathur, Michael A. Galella, Luisa Salter-Cid, Joel C. Barrish, Percy H. Carter, Aberra Fura, James R. Burke, and Joseph A. Tino

Cite This: *ACS Med. Chem. Lett.* 2020, 11, 2195–2203

Read Online

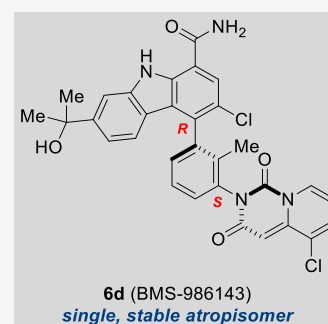
ACCESS |

Metrics & More

Article Recommendations

Supporting Information

ABSTRACT: Bruton's tyrosine kinase (BTK) has been shown to play a key role in the pathogenesis of autoimmunity. Therefore, the inhibition of the kinase activity of BTK with a small molecule inhibitor could offer a breakthrough in the clinical treatment of many autoimmune diseases. This Letter describes the discovery of BMS-986143 through systematic structure–activity relationship (SAR) development. This compound benefits from defined chirality derived from two rotationally stable atropisomeric axes, providing a potent and selective single atropisomer with desirable efficacy and tolerability profiles.



KEYWORDS: BTK, atropisomer, CD69, autoimmune disease

Protein kinases have been linked, directly and indirectly, to the pathophysiology of a large number of diseases.¹ Inhibition of kinase activity has the potential to interfere with critical signaling cascades, thus making kinases an attractive target for a wide variety of therapeutic areas.¹ One such protein kinase, Bruton's Tyrosine Kinase (BTK), is a nonreceptor kinase expressed in all hematopoietic cells including B cells, mast cells, and macrophages, but not in T cells or differentiated plasma cells. BTK, one of the five Tec family kinases, plays a crucial role in B cell receptor mediated signaling in B cells and Fcγ receptor (e.g., FcγRIIIa and FcγRIIIb) and Fcε receptor mediated signaling in myeloid cells.^{2–4} Autoimmune disease development in humans, including rheumatoid arthritis (RA) and lupus, is reliant on many of the BTK regulated signaling pathways.^{5–10} Consequently, the inhibition of the kinase activity of BTK has emerged as a clinical strategy for the treatment of many autoimmune diseases, without depleting B cells or inducing B cell immune deficiency.¹¹ This has led to a significant effort across the pharmaceutical industry to identify both irreversible and reversible small molecule inhibitors of BTK as clinical therapeutic agents to treat autoimmunity.^{12–26}

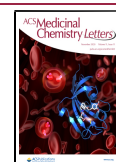
We previously disclosed a potent, reversible carbazole inhibitor of BTK (**1**, BTK IC₅₀ = 3 nM; human whole blood IC₅₀ = 550 nM measuring the expression of CD69). A notable characteristic was that **1** existed as a mixture of four

interconverting atropisomers. Although carbazole **1** demonstrated desirable efficacy in mouse models of RA, undesired side effects were noted during tolerability studies in multiple species. More recently, we reported on a strategy to improve the intrinsic activity, selectivity, and ultimately the tolerability profile through the identification of a single, stable atropisomer by rotationally locking two atropisomeric axes into the preferred bioactive conformation to inhibit BTK.²⁸ Removing the less target relevant atropisomers could potentially mitigate undesired off-target interactions that could be contributing to the toxicity observed with **1**. This was accomplished by replacing the quinazolinone with a quinazolinone to lock the lower atropisomeric axis and by adding small substituents at C3 to rotationally lock the carbazole C4 atropisomeric axis. This effort resulted in the identification of a single, rotationally stable atropisomer, carbazole **2**, which provided a 6-fold improvement in human whole blood potency when compared to **1** (IC₅₀ = 90

Received: June 16, 2020

Accepted: September 16, 2020

Published: September 16, 2020



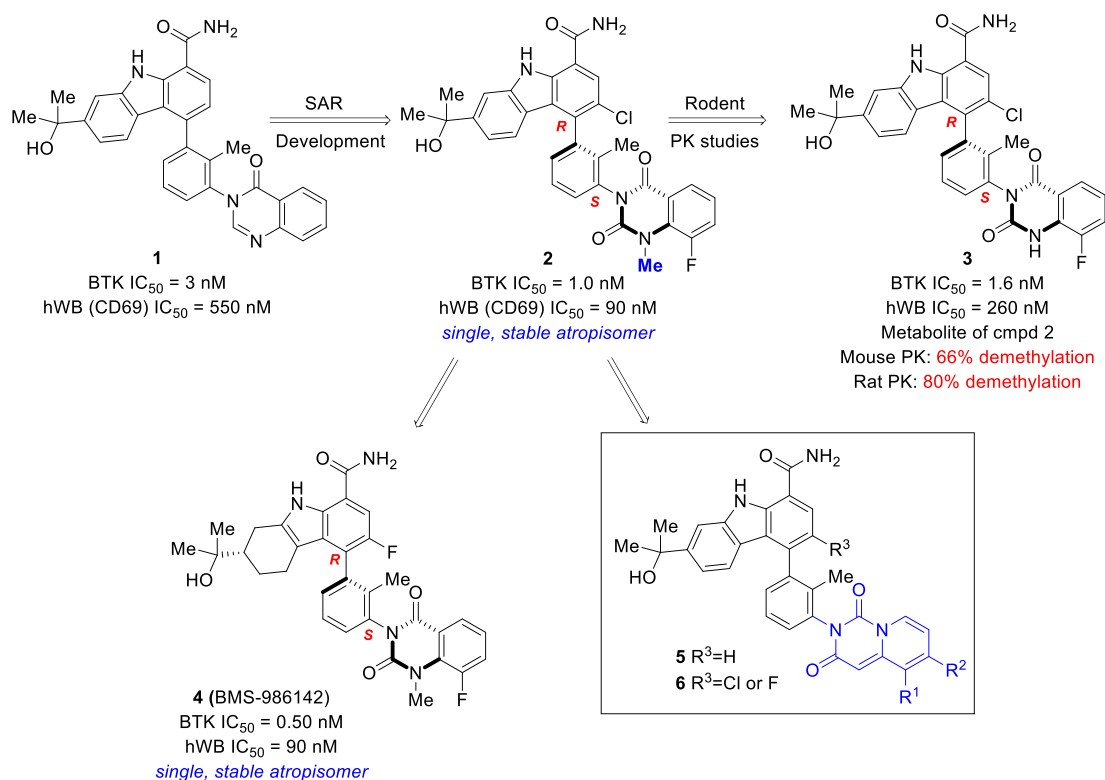


Figure 1. Identification of pyridopyrimidinedione inhibitors.

Table 1. In Vitro Potency of Carbazoles 5

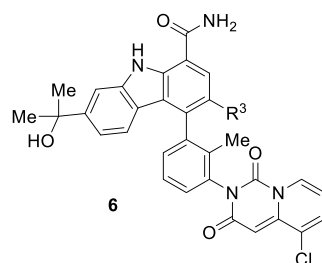
compd	in vitro activity							mouse PK (10 mg/kg)	
	dione chirality	R ¹	R ²	BTK IC ₅₀ (nM) ^a	JAK2/BTK selectivity	Ramos IC ₅₀ (nM) ^a	hWB IC ₅₀ (nM) ^a	C _{max} (μM)	AUC (μM·h)
1	NA	NA	NA	3.0 ± 0.10	94×	26 ± 15	550 ± 100	8.9	80
5a	peak 1	H	H	1.7 (n = 1)	1200×	19 ± 21	ND	0.54	2.5
5b	peak 2	H	H	1.8 (n = 1)	530×	8.5 ± 3.0	410 (n = 1)		
5c	racemate	H	OMe	0.63 (n = 1)	1600×	19 (n = 2)	140 (n = 1)	1.3	3.9
5d	racemate	OMe	H	0.52 (n = 1)	1900×	19 ± 10	140 ± 73	1.3	4.0
5e	racemate	H	Cl	0.49 ± 0.20	1500×	3.1 ± 2.7	3,000 (n = 3)		
5f	racemate	Cl	H	0.94 (n = 1)	1400×	12 (n = 2)	120 (n = 2)	3.5	23
5g	R	Cl	H	1.0 (n = 1)	1100×	18 (n = 1)	78 (n = 1)		
5h	S	Cl	H	0.41 (n = 2)	2500×	13 ± 7	69 (n = 2)		
5i	racemate	F	H	0.86 (n = 2)	1100×	19 (n = 2)	75 (n = 2)	5.2	28
5j	peak 1	F	H	1.7 (n = 2)	500×	18 (n = 2)	91 (n = 1)		
5k	peak 2	F	H	1.2 ± 0.8	870×	14 ± 1	79 ± 20		

^aIC₅₀ values are shown as mean values of at least three determinations unless specified otherwise; ND = not determined.

vs 550 nM), as well as improved kinase selectivity.²⁸ As previously disclosed, demethylation of the quinazolinone occurred in vivo in both mouse (66%) and rat (80%), resulting in the formation of metabolite 3.²⁸ Further structure–activity relationship (SAR) evolution, focused on exploring carbazole

C3 substitution as well as other structural variations, led to the identification of clinical asset BMS-986142 (4).^{28,29} In this letter, we outline a parallel strategy to overcome the stability issue through the replacement of the quinazolinone with pyridopyrimidinedione bicyclic systems 5 and 6 (Figure 1).

Table 2. In Vitro Potency of Carbazoles 6



compd	R ³	chirality	in vitro activity			
			BTK IC ₅₀ (nM) ^a	JAK2/BTK selectivity	Ramos IC ₅₀ (nM) ^a	hWB IC ₅₀ (nM) ^a
6a	Cl	homochiral	180 (n = 1)	11×	>300	ND
6b	Cl	homochiral	0.55 ± 0.16	2600×	10 ± 2	162 (n = 1)
6c	Cl	homochiral	17 (n = 1)	60×	87 (n = 1)	ND
6d	Cl	homochiral	0.26 ± 0.12	3800×	6.9 ± 3.4	25 ± 19
6e	F	homochiral	6.3 (n = 1)	330×	600 (n = 1)	ND
6f	F	homochiral	0.22 ± 0.07	6000×	6.6 ± 0.9	64 (n = 2)
6g	F	homochiral	7.2 (n = 1)	140×	170 (n = 2)	ND
6h	F	homochiral	0.19 ± 0.02	7200×	7.6 ± 2.4	37 (n = 2)

^aIC₅₀ values are shown as mean values of at least three determinations unless specified otherwise; ND = Not determined.

The pyridopyrimidinedione-carbazole compounds presented in this Letter were evaluated in both biochemical and cellular assays to determine their intrinsic activity against BTK (see Supporting Information S2). Enzymatic activity was established in a human recombinant BTK enzymatic assay.²⁸ Cellular activity was determined in a B cell receptor (BCR) stimulated calcium flux assay in Ramos B cells.²⁸ Potent analogues were then triaged with a human BCR stimulated whole blood assay (hWB), measuring the expression of CD69.²⁸ Additionally, compounds were evaluated against a subset of kinases with the goal of identifying a highly selective inhibitor. In this Letter, selectivity for BTK over JAK2 is shown in Tables 1 and 2, highlighting improved kinase selectivity relative to 1. Clinically, JAK2 inhibition has been associated with anemia,³⁰ a potentially undesirable side effect when considering the treatment of autoimmune disease. Select compounds, with desirable potency, selectivity, and in vitro liability profiles were subsequently evaluated in vivo.

As we initiated work in this series, compounds 5a and 5b (Table 1) were prepared from enantiomerically pure pyridopyrimidinedione atropisomeric intermediates, isolated from supercritical fluid chromatography (SFC) chiral resolution (see Supporting Information S1). Both compounds demonstrated comparable activity and selectivity when evaluated in the in vitro assays. Further SAR development focused on exploring substitution at the R¹ and R² positions to enhance potency. Since chiral resolution of the lower stable atropisomeric center did not result in significant differentiation, subsequent early compounds were evaluated as a racemic mixture of atropisomers at the dione and as a mixture of interconverting atropisomers at carbazole C4. The addition of a donating methoxy group at either the R¹ or R² carbons (5d and 5c) respectively, was tolerated, both providing very similar activity (BTK biochemical assay, the Ramos cellular assay, and the human whole blood assay) and similar oral plasma blood levels in mouse PK studies. Interestingly, both compounds were ~4-fold more potent in the whole blood assay when compared to compound 1 (140 vs 550 nM, respectively). Replacing the R² methoxy with a chloro (5e) maintained intrinsic activity; however, the compound was found

to be inactive in the whole blood assay (IC₅₀ > 3 μM). Further analysis revealed that 5e was unstable in whole blood when incubated at a concentration of 0.5 μM, showing >85% degradation within 10 min and complete degradation by the 2 h time point. To further understand the source of the instability, 5e was incubated in human liver microsomes with glutathione (10 μM, 60 min). The major metabolite identified corresponded to direct glutathione replacement of the pyridopyrimidinedione chloro substituent, indicating that the R² chloro is highly reactive. This is not surprising considering the δ-chloro enone motif. The R¹ chloro derivative (5f), on the other hand, was found to be stable in the same assay, and as a result was stable in the whole blood assay providing 120 nM activity. Enantiomerically pure chloro diones were prepared as stable atropisomers, derived from chiral boronic esters with confirmed absolute chirality. Both 5g (R) and 5h (S) provided ~7–8 fold improvement in whole blood potency relative to 1 and 13–27 fold improvement in the selectivity for BTK over JAK2. The R¹ fluoro substitution (5i–k) provided similar results. Although the systemic oral exposures in mouse PK for the compounds shown in Table 1 were lower than those seen with 1, we were encouraged by the significant improvement in human whole blood potency observed in this series.

The addition of either a chloro or a fluoro at the carbazole C3 position (R³) of compound 5i rotationally restricted the C3 atropisomeric center, allowing for the isolation of four single, stable atropisomeric compounds, as shown in Table 2. Although chloro versus fluoro substitution provided little differentiation in intrinsic potency, the chirality of the C4 individual atropisomers had a profound effect on potency and selectivity, with compound 6d providing a human whole blood IC₅₀ of 25 nM (22-fold more potent than 1) and selectivity for BTK over JAK2 of 3,800-fold (40-fold more selective than 1). Single crystal X-ray crystallographic analysis of compound 6d confirmed that the carbazole C4 atropisomer is the R configuration (Figure 2; CDCC # 1501157), consistent with the preferred bioactive conformation observed in the cocrystal structure of clinical asset BMS-986142 bound in the active site of BTK.²⁸ The lower dione atropisomer was confirmed to be the S configuration. When

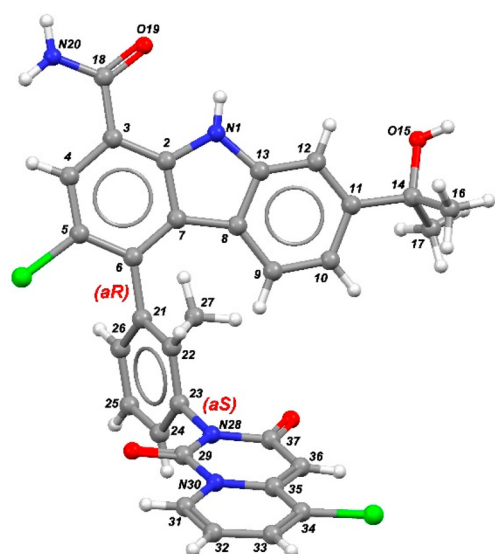


Figure 2. Single crystal X-ray structure of **6d** confirming the absolute atropisomeric stereochemistry (CDCC # 1501157).

comparing the desired, bioactive conformation (**6d**) with the undesired conformation (**6c**), the observed increase in biochemical, cellular, and human whole blood potencies, as well as the significant differences in the selectivity for BTK over JAK2, clearly demonstrates the potential benefit of preparing and isolating a single, rotationally stable atropisomeric compound. This effect is consistent with the benefits observed with traditional chiral center resolution. It is worth noting that both atropisomers **6c** and **6d** showed similar inhibition of JAK2 with an IC_{50} of $\sim 1 \mu M$, so the improvement in selectivity observed is derived from the increased affinity of **6d** for BTK. With highly desirable whole blood potency and selectivity, **6d** was advanced for further evaluation.

A more in depth in vitro activity profile for **6d** is presented in Table 3. In multiple assays aimed at establishing the effectiveness of the compound in inhibiting critical B cell functions derived through BCR stimulation, including proliferation, antibody production, and costimulatory molecule expression, **6d** potently inhibited signaling and functional end points with single digit nanomolar activity. Consistent with the inhibition observed in BCR stimulated pathways, **6d** provided potent inhibition of end points derived from IgG-containing immune complex low affinity activating $Fc\gamma$ receptor signaling in peripheral blood mononuclear cells (PBMC) ($IC_{50} = 2 \text{ nM}$). Of particular interest, **6d** inhibited the expression of CD63 on the surface of basophils in human whole blood, driven by $Fc\epsilon R1$ signaling (IC_{50} of 54 nM). This is similar to the previously stated human whole blood activity when measuring the BCR-stimulated expression of CD69 on the surface of B cells ($IC_{50} = 25 \text{ nM}$). Compared to our early lead compound **1** (Table 3), **6d** provided significantly enhanced cellular and whole blood potencies.

Carbazole **6d** was evaluated against 384 kinases, inhibiting only seven kinases with less than 100-fold selectivity relative to BTK (Table 4). Four of the seven were Tec family members, TEC, BMX, TXK, and ITK, and only three kinases, TEC, BLK, and BMX, were inhibited with less than 30-fold selectivity relative to BTK.

In pharmacokinetic (PK) studies in mice and dogs (Table 5), carbazole **6d** was highly absorbed with bioavailability of 100%

Table 3. Partial In Vitro Cell Activity Data and Whole Blood Data for 6d

assay	receptor/stimulation	IC_{50} (nM) ^a	
		6d	1
cellular assays			
calcium flux in Ramos B Cells	BCR/anti-IgM	7 ± 3	26 ± 15
proliferation of human peripheral B Cells	BCR/anti-IgM/IgG	1 ± 0.4	8 ^b
CD86 surface expression in peripheral B Cells	BCR/anti-IgM/IgG	1 ± 0.5	40 ± 30
CD86 surface expression in peripheral B Cells	CD40/CD40L	>10 000	>10 000
TNF α from human PBMC Cells	FC γ R/immune complex	2 ^b	14 ^b
human whole blood assays			
human whole blood CD69 surface expression in peripheral B Cells	BCR/anti-IgM	25 ± 10	550 ± 100
mouse whole blood CD69 surface expression in peripheral B Cells	BCR/anti-IgM/IgG	130	2,100 ± 200
human whole blood CD63 surface expression in basophils	Fc ϵ RI/anti-IgE	54 ± 20	ND

^a IC_{50} values are shown as mean values of at least three determinations. ^b IC_{50} values are shown as a single determination; PBMC = peripheral blood mononuclear cells; ND = not determined.

Table 4. Partial In Vitro Selectivity Data for 6d

kinase	biochemical IC_{50} (nM)	kinase/BTK fold selectivity
BTK (Tec family)	0.26	
TEC (Tec family)	3	10×
BLK	5	17×
BMX (Tec family)	7	23×
TXK (Tec family)	10	33×
FGR	15	50×
YES1	19	63×
ITK (Tec family)	21	70×

and 82%, respectively. The compound had a low rate of plasma clearance with a large steady-state volume of distribution in both species. On the basis of the PK and liability profiles (Table 6), coupled with demonstrated potency and selectivity, **6d** was further evaluated in vivo in models of human RA.

In order to understand the compounds impact on in vivo efficacy in models of human RA, **6d** was evaluated in two mouse models, a collagen-induced arthritis (CIA) model,¹⁹ dependent on both BCR-signaling and $Fc\gamma$ receptor signaling, and an anticollagen antibody-induced model,²⁸ dependent solely on $Fc\gamma$ receptor signaling. In the CIA study (Figure 3), **6d** was dosed orally at 15 and 45 mg/kg BID and provided dose-dependent inhibition of observed clinical disease progression (63% and 80%, respectively), representing 17 and 19 h coverage of the mouse whole blood IC_{50} (130 nM). In the anticollagen

Table 5. Pharmacokinetic Parameters for 6d

parameter	mouse ^b	dog ^a
po dose (mg/kg)	6	2
iv dose (mg/kg)	3	1
C _{max} (μM), PO	4.3	1.2 ± 0.4
T _{max} (μM), PO	1.0	3.7 ± 1.2
AUC (μM·h), PO	20	13 ± 6
T _{1/2} (h), iv	3.6	7.9 ± 0.6
MRT (h), iv	3.5	10.1 ± 1.5
CL (mL/min/kg), iv	8.6	4.4 ± 0.7
V _{ss} (L/kg), iv	1.8	2.6 ± 0.3
F _{po} (%)	100	82 ± 31

^aAverage of three animals. ^bAverage of two animals. Vehicle: (po) 80% PEG400, 20% water; (iv) 10% DMAC, 30% PEG300, 60% water; (iv dog) 10% EtOH, 70% PEG400, 20% water.

Table 6. Partial In Vitro Profiling Data for 6d

parameter	result
protein binding (bound)	99.7% human 99.4% mouse 99.5% rat 98.7% dog 98.2% monkey
mutagenicity	Ames negative
hERG (patch clamp)	IC ₅₀ > 30 μM
Na ⁺ (patch clamp)	13% @ 10 μM (1 and 4 Hz)
Ca ⁺ (patch clamp)	19% @ 10 μM
CYP inhibition (IC ₅₀) ^a	>12 μM 1A2, 2B6, 2D6, 2C19 3.2 μM 2C8 5.7 μM 2C9 11 μM 3A4
PAMPA permeability	1836/1302 nm/s (pH 5.5/7.4)
Caco2 Permeability:	ND due to insufficient recovery
Aqueous solubility	<0.001 mg/mL
FaSSIF solubility ^b	14 μg/mL
FeSSIF solubility ^c	551 μg/mL
log D at pH 7.0 (HPLC)	3.84

^aCYP = Cytochrome P450. ^bFaSSIF = Fasted state simulated intestinal fluid. ^cFeSSIF = Fed state simulated intestinal fluid; ND = not determined.

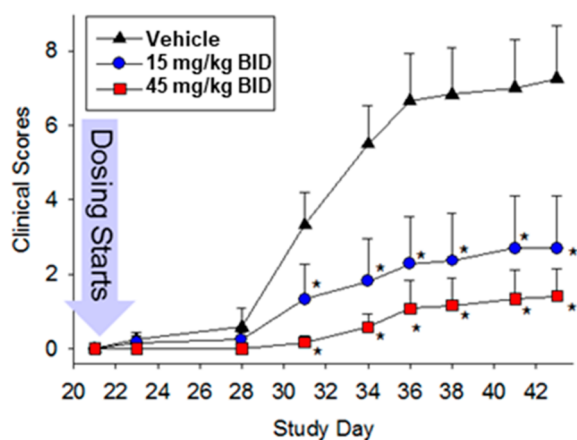


Figure 3. Efficacy of 6d in mouse model of human collagen-induced arthritis. A 15 mg/kg BID dose provided 17 h coverage of the mouse WB IC₅₀ (130 nM) while a 45 mg/kg BID dose provided 19 h coverage. Error bars represent the mean ± SEM. *P < 0.05 versus vehicle control group.

antibody-induced arthritis (CAIA) study (Figure 4), 6d when dosed orally at 10 and 25 mg/kg BID resulted in 78% and 100% suppression of clinically evident paw swelling, respectively. The observed efficacy corresponded to 17 h (10 mg/kg BID) and 23 h (25 mg/kg BID) coverage of the mouse whole blood IC₅₀ (130 nM). In summary, PK/PD relationships for 6d in preclinical models of arthritis suggested that coverage of the whole blood IC₅₀ for 18 h duration is needed to achieve robust efficacy of >70% reduction in clinical scores. Doses providing close to 24 h duration of whole blood IC₅₀ coverage resulted in maximal efficacy (100% reductions in clinical scores).

Compounds represented by pyridopyrimidinediones 5³¹ and 6³² were prepared as outlined in Schemes 1–3. The final compounds were synthesized as shown in Scheme 1. Carbazole 7^{27,28} was coupled with the appropriate pyridopyrimidinedione (8) under standard Suzuki coupling conditions³³ to give the racemic compounds 5 and 9. If R³ is Cl or F, subsequent SFC chiral resolution provided each of the four rotationally stable atropisomers 6a–h. Alternatively, compounds 5g, 5h, and 6d were prepared starting with the appropriate chiral boronic ester 10 or 16, as depicted in Scheme 2. The absolute chiral configuration of 6d was established through single crystal X-ray structural elucidation (Figure 2; CDCC # 1501157).

The synthesis of boronic ester intermediates 8, 10, and 16 is shown in Scheme 3. Commercially available phenyl acetic acids or sodium salts prepared as outlined in Scheme 3 were coupled with 3-bromo-2-methylaniline in the presence of HATU and diisopropylamine in DMF to give 14. Intermediate 14 was converted to boronic ester 15, which was subsequently heated with carbondiimidazole in toluene at 100 °C to provide 8. SFC chiral resolution afforded single, rotationally stable atropisomeric intermediates 10 and 16. The absolute configuration of boronic ester 10 was confirmed to be S through single crystal X-ray structural elucidation (CDCC # 1501156; refer to the supplemental section for structural details).

The inhibition of the kinase activity of BTK with a small molecule inhibitor has emerged as a clinical strategy for the treatment of many autoimmune diseases. Pyridopyrimidinedione-carbazoles were envisioned to resolve a metabolic stability issue observed in the quinazolinone series. An iterative SAR effort established the viability of the pyridopyrimidinediones as a

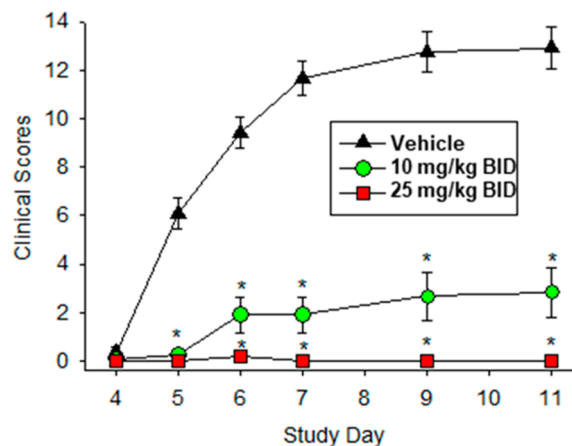
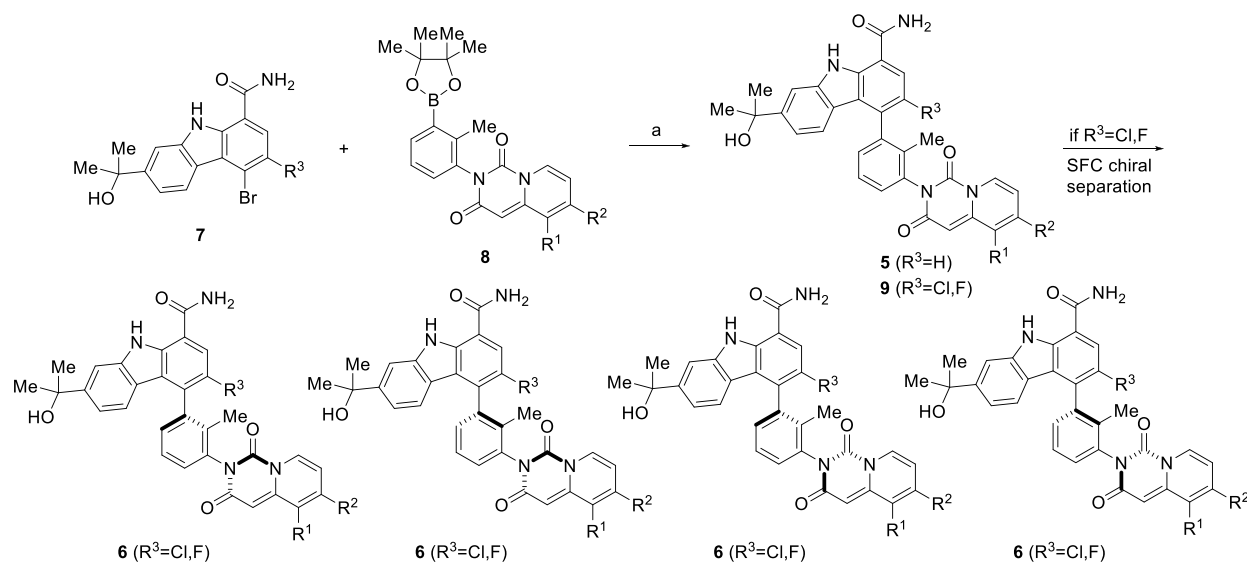
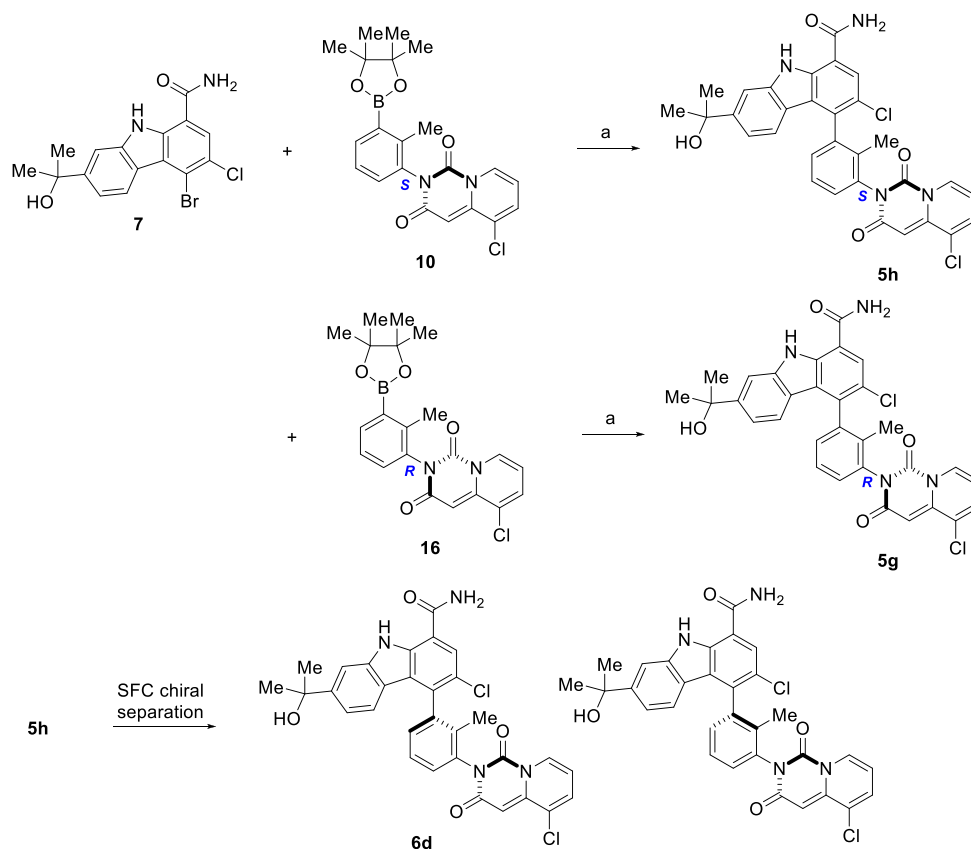


Figure 4. Efficacy of 6d in FcγR-dependent collagen Ab-induced arthritis (CAIA). Robust efficacy was observed with a 10 mg/kg BID dose providing 18 h coverage of the mouse WB IC₅₀ (130 nM), and a 25 mg/kg BID dose provided 23 h coverage. Error bars represent the mean ± SEM. *P < 0.05 versus vehicle control group.

Scheme 1. Preparation of Carbazoles 5, 6, and 9^a

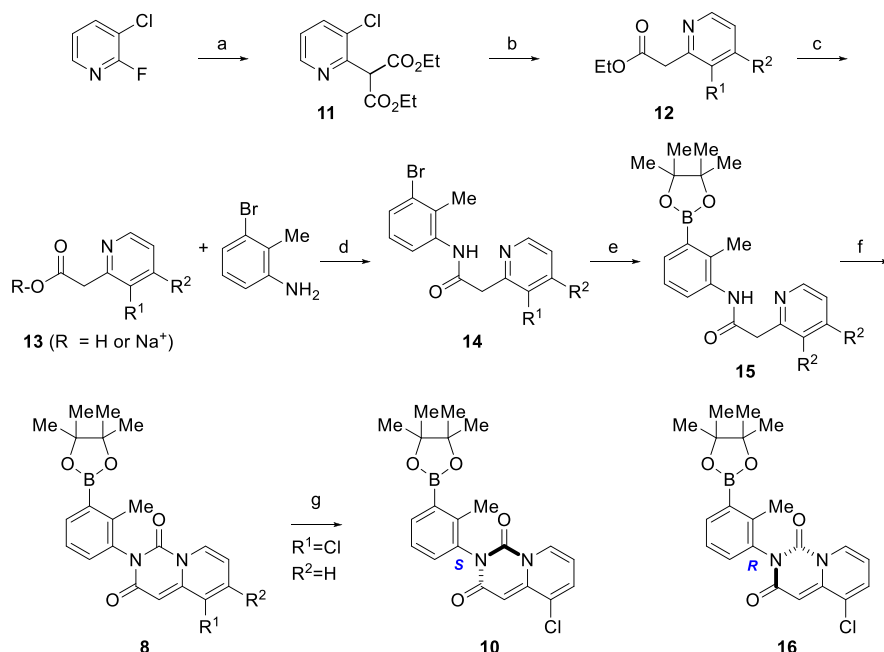
^aReagents and conditions: (a). Dichloro 1,1'-bis(diphenylphosphino)ferrocene palladium(II)-CH₂Cl₂ adduct, Cs₂CO₃, THF-water, 45 °C, 60–65% yield.

Scheme 2. Preparation of Atropisomers 5g and 5h and Preparation of Single, Rotationally Stable Atropisomer 6d^a

^aReagents and conditions: (a). Dichloro 1,1'-bis(diphenylphosphino)ferrocene palladium(II)-CH₂Cl₂ adduct, Cs₂CO₃, THF-water, 45 °C; 60–68% yield.

progressable series. This effort resulted in the identification of a single atropisomer **6d**, conformationally stable under physiological conditions, which demonstrated significant improvements in human whole blood potency (25 versus 550 nM, respectively) and overall selectivity relative to earlier lead **1**.

Importantly, in multiple species, carbazole **6d** had a desirable safety and tolerability profile. This clearly demonstrates the potential benefit of preparing and isolating a single, rotationally stable atropisomeric compound to enhance potency, selectivity, and safety, similar to the benefits observed with traditional chiral

Scheme 3. Preparation of Boronic Esters Intermediates 8, 10, and 17^a

^aReagents and conditions: (a) Diethyl malonate, Cs₂CO₃, DMSO, 100 °C; (b) NaCl, H₂O, DMSO, 145 °C; (c) 3N NaOH, THF, rt.; (d) DIEA, HATU, DMF, rt., 89% yield over 4 steps; (e) DIBALCO, dichloro 1,1'-bis(diphenylphosphino)ferrocene palladium(II)-CH₂Cl₂ adduct, potassium acetate, DMSO, 90 °C, 85%; (f) CDI, Toluene, 110 °C, 65% yield; (g) SFC chiral separation.

center resolution. With a desirable in vitro and in vivo profile, 3-chloro-4-(*R*)-(3-(*S*)-(5-chloro-1,3-dioxo-1*H*-pyrido[1,2-*c*]pyrimidin-2(3*H*)-yl)-2-methylphenyl)-7-(2-hydroxypropan-2-yl)-9*H*-carbazole-1-carboxamide (**6d**, BMS-986143) was selected as a development candidate for further evaluation as a potential agent for the treatment of autoimmune diseases.

■ ASSOCIATED CONTENT

Supporting Information

The Supporting Information is available free of charge at <https://pubs.acs.org/doi/10.1021/acsmchemlett.0c00335>.

Experimental details and compound characterization data for key compounds as well as biological protocols (PDF)

■ AUTHOR INFORMATION

Corresponding Authors

Anurag S. Srivastava – Bristol Myers Squibb Research and Early Development, Princeton, New Jersey 08543, United States;
Email: anuragsrivastava152@gmail.com

Scott H. Watterson – Bristol Myers Squibb Research and Early Development, Princeton, New Jersey 08543, United States;
 orcid.org/0000-0001-9315-177X;
Email: scott.watterson@bms.com

Authors

Soo Ko – Bristol Myers Squibb Research and Early Development, Princeton, New Jersey 08543, United States

Mark A. Pattoli – Bristol Myers Squibb Research and Early Development, Princeton, New Jersey 08543, United States

Stacey Skala – Bristol Myers Squibb Research and Early Development, Princeton, New Jersey 08543, United States

Lihong Cheng – Bristol Myers Squibb Research and Early Development, Princeton, New Jersey 08543, United States

Mary T. Obermeier – Bristol Myers Squibb Research and Early Development, Princeton, New Jersey 08543, United States

Rodney Vickery – Bristol Myers Squibb Research and Early Development, Princeton, New Jersey 08543, United States

Lorell N. Discenza – Bristol Myers Squibb Research and Early Development, Princeton, New Jersey 08543, United States

Celia J. D'Arienzo – Bristol Myers Squibb Research and Early Development, Princeton, New Jersey 08543, United States

Kathleen M. Gillooly – Bristol Myers Squibb Research and Early Development, Princeton, New Jersey 08543, United States

Tracy L. Taylor – Bristol Myers Squibb Research and Early Development, Princeton, New Jersey 08543, United States

Claudine Pulicchio – Bristol Myers Squibb Research and Early Development, Princeton, New Jersey 08543, United States

Kim W. McIntyre – Bristol Myers Squibb Research and Early Development, Princeton, New Jersey 08543, United States

Shiuhang Yip – Bristol Myers Squibb Research and Early Development, Princeton, New Jersey 08543, United States

Peng Li – Bristol Myers Squibb Research and Early Development, Princeton, New Jersey 08543, United States

Dawn Sun – Bristol Myers Squibb Research and Early Development, Princeton, New Jersey 08543, United States

Dauh-Rung Wu – Bristol Myers Squibb Research and Early Development, Princeton, New Jersey 08543, United States

Jun Dai – Bristol Myers Squibb Research and Early Development, Princeton, New Jersey 08543, United States

Chunlei Wang – Bristol Myers Squibb Research and Early Development, Princeton, New Jersey 08543, United States

Yingru Zhang – Bristol Myers Squibb Research and Early Development, Princeton, New Jersey 08543, United States

Bei Wang – Bristol Myers Squibb Research and Early Development, Princeton, New Jersey 08543, United States

Joseph Pawluczyk – Bristol Myers Squibb Research and Early Development, Princeton, New Jersey 08543, United States

James Kempson – Bristol Myers Squibb Research and Early Development, Princeton, New Jersey 08543, United States;

orcid.org/0000-0002-9540-3886

Rulin Zhao – Bristol Myers Squibb Research and Early Development, Princeton, New Jersey 08543, United States

Xiaoping Hou – Bristol Myers Squibb Research and Early Development, Princeton, New Jersey 08543, United States;

orcid.org/0000-0001-6169-3443

Richard Rampulla – Bristol Myers Squibb Research and Early Development, Princeton, New Jersey 08543, United States

Arvind Mathur – Bristol Myers Squibb Research and Early Development, Princeton, New Jersey 08543, United States

Michael A. Galella – Bristol Myers Squibb Research and Early Development, Princeton, New Jersey 08543, United States

Luisa Salter-Cid – Bristol Myers Squibb Research and Early Development, Princeton, New Jersey 08543, United States

Joel C. Barrish – Bristol Myers Squibb Research and Early Development, Princeton, New Jersey 08543, United States

Percy H. Carter – Bristol Myers Squibb Research and Early Development, Princeton, New Jersey 08543, United States

Aberra Fura – Bristol Myers Squibb Research and Early Development, Princeton, New Jersey 08543, United States

James R. Burke – Bristol Myers Squibb Research and Early Development, Princeton, New Jersey 08543, United States

Joseph A. Tino – Bristol Myers Squibb Research and Early Development, Princeton, New Jersey 08543, United States

Complete contact information is available at:

<https://pubs.acs.org/10.1021/acsmmedchemlett.0c00335>

Notes

The authors declare no competing financial interest.

ACKNOWLEDGMENTS

We would like to thank our colleagues in the Department of Discovery Synthesis at the Biocon-BMS Center (Bengaluru, India) for their contributions toward intermediate preparation.

ABBREVIATIONS

BTK, Bruton's tyrosine kinase; PK, pharmacokinetic; SAR, structure–activity relationship; hERG, human ether-a-go-go-related gene.

REFERENCES

- Zhang, J.; Yang, P. L.; Gray, N. S. Targeting cancer with small molecule kinase inhibitors. *Nat. Rev. Cancer* **2009**, *9*, 28–39.
- Mohamed, A. J.; Yu, L.; Bäckesjö, C.-M.; Vargas, L.; Faryal, R.; Aints, A.; Christensson, B.; Berglöf, A.; Vihinen, M.; Nore, B. F.; Smith, C. I. E. Bruton's tyrosine kinase (Btk): function, regulation, and transformation with special emphasis on the PH domain. *Immunol. Rev.* **2009**, *228*, 58–73.
- Mohamed, A. J.; Nore, B. F.; Christensson, B.; Smith, C. I. E. Signaling of Bruton's tyrosine kinase, Btk. *Scand. J. Immunol.* **1999**, *49*, 113–118.
- Takata, M.; Kurosaki, T. A role for Bruton's tyrosine kinase in B cell antigen receptor-mediated activation of phospholipase C- γ 2. *J. Exp. Med.* **1996**, *184*, 31–40.
- Jansson, L.; Holmdahl, R. Genes on the X chromosome affect development of collagen-induced arthritis in mice. *Clin. Exp. Immunol.* **1993**, *94*, 459–465.
- Steinberg, B. J.; Smathers, P. A.; Frederiksen, K.; Steinberg, A. D. Ability of the *xid* gene to prevent autoimmunity in (NZBXNZW)F1 mice during the course of their natural history, after polyclonal stimulation, or following immunization with DNA. *J. Clin. Invest.* **1982**, *70*, 587–597.
- Xu, D.; Kim, Y.; Postelnek, J.; Vu, M. D.; Hu, D.-Q.; Liao, C.; Bradshaw, M.; Hsu, J.; Zhang, J.; Pashine, A.; Srinivasan, D.; Woods, J.; Levin, A.; O'Mahony, A.; Owens, T. D.; Lou, Y.; Hill, R. J.; Narula, S.; DeMartino, J.; Fine, J. S. RN486, a selective Bruton's tyrosine kinase inhibitor, abrogates immune hypersensitivity responses and arthritis in rodents. *J. Pharmacol. Exp. Ther.* **2012**, *341*, 90–103.
- Di Paolo, J. A.; Huang, T.; Balazs, M.; Barbosa, J.; Barck, K. H.; Bravo, B. J.; Carano, R. A. D.; Darrow, J.; Davies, D. R.; DeForge, L. E.; Diehl, L.; Ferrando, R.; Gallion, S. L.; Giannetti, A. M.; Gribling, P. P.; Hurez, V.; Hymowitz, S. G.; Jones, R.; Kropf, J. E.; Lee, W. P.; Maciejewski, P. M.; Mitchell, S. A.; Rong, H.; Staker, B. L.; Whitney, J. A.; Yeh, S.; Young, W. B.; Yu, C.; Zhang, J.; Reif, K.; Currie, K. S. Specific Btk inhibition suppresses B cell and myeloid cell-mediated arthritis. *Nat. Chem. Biol.* **2011**, *7*, 41–50.
- Rankin, A. L.; Seth, N.; Keegan, S.; Andreyeva, T.; Cook, T. A.; Edmonds, J.; Mathialagan, N.; Benson, M. J.; Syed, J.; Zhan, Y.; Benoit, S. E.; Miyashiro, J. S.; Wood, N.; Mohan, S.; Peeva, E.; Ramaiah, S. K.; Messing, D.; Homer, B. L.; Dunussi-Joannopoulos, K.; Nickerson-Nutter, C. L.; Schnute, M. E.; Douhan, J., III. Selective inhibition of BTK prevents murine lupus and antibody-mediated glomerulonephritis. *J. Immunol.* **2013**, *191*, 4540–4550.
- Mease, P. J. B cell-targeted therapy in autoimmune disease: rationale, mechanisms, and clinical application. *J. Rheumatol.* **2008**, *35*, 1245–1255.
- Crofford, L. J.; Nyhoff, L. E.; Sheehan, J. H.; Kendall, P. L. The role of Bruton's tyrosine kinase in autoimmunity and implications for therapy. *Expert Rev. Clin. Immunol.* **2016**, *12*, 763–773.
- Crawford, J. J.; Johnson, A. R.; Misner, D. L.; Belmont, L. D.; Castanedo, G.; Choy, R.; Coraggio, M.; Dong, L.; Eigenbrot, C.; Erickson, R.; Ghilardi, N.; Hau, J.; Katewa, A.; Kohli, P. B.; Lee, W.; Lubach, J. W.; McKenzie, B. S.; Ortwine, D. F.; Schutt, L.; Tay, S.; Wei, B.-Q.; Reif, K.; Liu, L.; Wong, H.; Young, W. B. Discovery of GDC-0853: A potent, selective, and noncovalent Bruton's tyrosine kinase inhibitor in early development. *J. Med. Chem.* **2018**, *61*, 2227–2245.
- Cohen, S.; Tuckwell, K.; Zhao, R.; Galanter, J.; Lee, C.; Rae, J.; Toth, B.; Ramamoorthi, N.; Hackney, J. A.; Chinn, L. W.; Townsend, M. J.; Morimoto, A. M.; Katsumoto, T. R.; Genovese, M. C.; Berman, A.; Damjanov, N.; Fedkov, D.; Jeka, S.; et al. Fenebrutinib versus placebo or adalimumab in rheumatoid arthritis: A randomized, double-blind, phase II trial (ANDES Study). *Arthritis Rheumatol.* **2020**, *72*, 1435.
- Caldwell, R. D.; Qiu, H.; Askew, B. C.; Bender, A. T.; Brugger, N.; Camps, M.; Dhanabal, M.; Dutt, V.; Eichhorn, T.; Gardberg, A. S.; Goutopoulos, A.; Grenningloh, R.; Head, J.; Healey, B.; Hodous, B. L.; Huck, B. R.; Johnson, T. L.; Jones, C.; Jones, R. C.; Mochalkin, I.; Morandi, F.; Nguyen, N.; Meyring, M.; Potnick, J. R.; Santos, D. C.; Schmidt, R.; Sherer, B.; Shutes, A.; Urbahns, K.; Follis, A. V.; Wegener, A. A.; Zimmerli, S. C.; Liu-Bujalski, L. Discovery of evobrutinib: An oral, potent, and highly selective, covalent Bruton's tyrosine kinase (BTK) inhibitor for the treatment of immunological diseases. *J. Med. Chem.* **2019**, *62*, 7643–7655.
- Montalban, X.; Arnold, D. L.; Weber, M. S.; Staikov, I.; Piasecka-Stryczynska, K.; Willmer, J.; Martin, E. C.; Dangond, F.; Syed, S.; Wolinsky, J. S. Placebo-controlled trial of an oral BTK inhibitor in multiple sclerosis. *N. Engl. J. Med.* **2019**, *380*, 2406–2417.
- Smith, P. F.; Krishnarajah, J.; Nunn, P. A.; Hill, R. J.; Karr, D.; Tam, D.; Masjedzadeh, M.; Funk, J. O.; Gourlay, S. G. A phase I trial of PRN1008, a novel reversible covalent inhibitor of Bruton's tyrosine kinase, in healthy volunteers. *Br. J. Clin. Pharmacol.* **2017**, *83*, 2367–2376.
- Hill, R. J.; Smith, P.; Krishnarajah, J.; Bradshaw, J. M.; Masjedzadeh, M.; Bisconte, A.; Karr, D.; Owens, T. D.; Brameld, K.; Funk, J. O.; Goldstein, D. M.; Nunn, P. A.; Gourlay, S. G. Discovery of PRN1008, a novel, reversible covalent BTK inhibitor in clinical development for rheumatoid arthritis. *Arthritis Rheumatol.* **2015**, *67* (suppl 10). <https://acrabstracts.org/abstract/discovery-of-prn1008-a-novel-reversible-covalent-btk-inhibitor-in-clinical-development-for-rheumatoid-arthritis/>.

(18) Smith, P. F.; Owens, T. D.; Langrish, C. L.; Xing, Y.; Francesco, M. R.; Shu, J.; Hartmann, S.; Karr, D.; Burns, R.; Quesenberry, R.; Neale, A.; Gourlay, S. G.; Redfern, A. Discovery of PRN1008, a novel, reversible covalent BTK inhibitor in clinical development for rheumatoid arthritis. *ACTRIMS* **2019**, No. 3790.

(19) Watterson, S. H.; Liu, Q.; Beaudoin Bertrand, M.; Batt, D. G.; Li, L.; Pattoli, M. A.; Skala, S.; Cheng, L.; Obermeier, M. T.; Moore, R.; Yang, Z.; Vickery, R.; Elzinga, P. A.; Discenza, L.; D'Arienzo, C.; Gillooly, K. M.; Taylor, T. L.; Pulicicchio, C.; Zhang, Y.; Heimrich, E.; McIntyre, K. W.; Ruan, Q.; Westhouse, R. A.; Catlett, I. M.; Zheng, N.; Chaudhry, C.; Dai, J.; Galella, M. A.; Tebben, A. J.; Pokross, M.; Li, J.; Zhao, R.; Smith, D.; Rampulla, R.; Allentoff, A.; Wallace, M. A.; Mathur, A.; Salter-Cid, L.; Macor, J. E.; Carter, P. H.; Fura, A.; Burke, J. R.; Tino, J. A. Discovery of Branebrutinib (BMS-986195): A strategy for identifying a highly potent and selective covalent inhibitor providing rapid in vivo inactivation of Bruton's tyrosine kinase (BTK). *J. Med. Chem.* **2019**, *62*, 3228–3250.

(20) Catlett, I. M.; Nowak, M.; Kundu, S.; Zheng, N.; Liu, A.; He, B.; Girgis, I. G.; Grasela, D. M. Safety, pharmacokinetics and pharmacodynamics of branebrutinib (BMS-986195), a covalent, irreversible inhibitor of Bruton's tyrosine kinase: Randomised phase I, placebo-controlled trial in healthy participants. *Br. J. Clin. Pharmacol.* **2020**, *86*, 1849.

(21) Evans, E. K.; Tester, R.; Aslanian, S.; Karp, R.; Sheets, M.; Labenski, M. T.; Witowski, S. R.; Lounsbury, H.; Chaturvedi, P.; Mazdiyasi, H.; Zhu, Z.; Nacht, M.; Freed, M. I.; Petter, R. C.; Dubrovsky, A.; Singh, J.; Westlin, W. F. Inhibition of BTK with CC-292 provides early pharmacodynamic assessment of activity in mice and humans. *J. Pharmacol. Exp. Ther.* **2013**, *346*, 219–228.

(22) Schafer, P. H.; Kivitz, A. J.; Ma, J.; Korish, S.; Sutherland, D.; Li, L.; Azaryan, A.; Kosek, J.; Adams, M.; Capone, L.; Hur, E. M.; Hough, D. R.; Ringheim, G. E. Spebrutinib (CC-292) affects markers of B cell activation, chemotaxis, and osteoclasts in patients with rheumatoid arthritis: Results from a mechanistic study. *Rheumatol. Thera.* **2020**, *7*, 101–119.

(23) Park, J. K.; Byun, J.-Y.; Park, J. A.; Kim, Y.-Y.; Lee, Y. J.; Oh, J. I.; Jang, S. Y.; Kim, Y. H.; Song, Y. W.; Son, J.; Suh, K. H.; Lee, Y.-M.; Lee, E. B. HM71224, a novel Bruton's tyrosine kinase inhibitor, suppresses B cell and monocyte activation and ameliorates arthritis in a mouse model: a potential drug for rheumatoid arthritis. *Arthritis Res. Ther.* **2016**, *18*, 91–1.

(24) Goess, C.; Harris, C. M.; Murdock, S.; McCarthy, R. W.; Sampson, E.; Twomey, R.; Mathieu, S.; Mario, R.; Perham, M.; Goedken, E. R.; Long, A. J. ABBV-105, a selective and irreversible inhibitor of Bruton's tyrosine kinase, is efficacious in multiple preclinical models of inflammation. *Mod. Rheumatol.* **2019**, *29*, 510–522.

(25) Angst, D.; Gessier, F.; Janser, P.; Vulpetti, A.; Walchli, R.; Beerli, C.; Littlewood-Evans, A.; Dawson, J.; Nuesslein-Hildesheim, B.; Wiczorek, G.; Gutmann, S.; Scheufler, C.; Hinniger, A.; Zimmerlin, A.; Funhoff, E. G.; Pulz, R.; Cenni, B. Discovery of LOU064 (remibrutinib), a potent and highly selective covalent inhibitor of Bruton's tyrosine kinase. *J. Med. Chem.* **2020**, *63*, 5102.

(26) Hosoi, F.; Iguchi, S.; Yoshiga, Y.; Kaneko, R.; Nakachi, Y.; Akasaka, D.; Yonekura, K.; Iwasawa, Y.; Sasaki, E.; Utsugi, T. OP0075 TASS315, A novel Bruton's tyrosine kinase (BTK) inhibitor, demonstrates potent efficacy in mouse collagen-induced arthritis model. *Ann. Rheum. Dis.* **2015**, *74*, 97.1.

(27) De Lucca, G. B.; Shi, Q.; Liu, Q.; Batt, D. G.; Bertrand, M. B.; Rampulla, R.; Mathur, A.; Discenza, L.; D'Arienzo, C.; Dai, J.; Obermeier, M. T.; Vickery, R.; Zhang, Y.; Yang, Z.; Marathe, P. H.; Tebben, A. J.; Muckelbauer, J. K.; Chang, C. Y.; Zhang, H.; Gillooly, K.; Taylor, T. L.; Pattoli, M. A.; Skala, S.; Kukral, D. W.; McIntyre, K. W.; Salter-Cid, L.; Fura, A.; Burke, J. R.; Barrish, J. C.; Carter, P. H.; Tino, J. A. Small molecule reversible inhibitors of Bruton's tyrosine Kinase (BTK): Structure-activity relationships leading to the identification of 7-(2-hydroxypropan-2-yl)-4-[2-methyl-3-(4-oxo-3,4-dihydroquinazolin-3-yl)phenyl]-9H-carbazole-1-carboxamide (BMS-935177). *J. Med. Chem.* **2016**, *59*, 7915–7935.

(28) Watterson, S. H.; Liu, Q.; Beaudoin Bertrand, M.; Batt, D. G.; Li, L.; Pattoli, M. A.; Skala, S.; Cheng, L.; Obermeier, M. T.; Moore, R.; Yang, Z.; Vickery, R.; Elzinga, P. A.; Discenza, L.; D'Arienzo, C.; Gillooly, K. M.; Taylor, T. L.; Pulicicchio, C.; Zhang, Y.; Heimrich, E.; McIntyre, K. W.; Ruan, Q.; Westhouse, R. A.; Catlett, I. M.; Zheng, N.; Chaudhry, C.; Dai, J.; Galella, M. A.; Tebben, A. J.; Pokross, M.; Li, J.; Zhao, R.; Smith, D.; Rampulla, R.; Allentoff, A.; Wallace, M. A.; Mathur, A.; Salter-Cid, L.; Macor, J. E.; Carter, P. H.; Fura, A.; Burke, J. R.; Tino, J. A. Discovery of Branebrutinib (BMS-986195): A strategy for identifying a highly potent and selective covalent inhibitor providing rapid in vivo inactivation of Bruton's tyrosine kinase (BTK). *J. Med. Chem.* **2019**, *62*, 3228–3250.

(29) Lee, S. K.; Xing, J.; Catlett, I. M.; Adamczyk, R.; Griffies, A.; Liu, A.; Murthy, B.; Nowak, M. Safety, pharmacokinetics, and pharmacodynamics of BMS-986142, a novel reversible BTK inhibitor, in healthy participants. *Eur. J. Clin. Pharmacol.* **2017**, *73*, 689–698.

(30) Winton, E. F.; Kota, V. Mometinib in myelofibrosis: JAK1/2 inhibitor with a role in treating and understanding anemia. *Future Oncol.* **2017**, *13*, 395–407.

(31) Ko, S. S.; Batt, D. A.; Bertrand, M. B.; Delucca, G. V.; Langevine, C. M.; Liu, Q.; Srivastava, A. S.; Watterson, S. H. Carbazole carboxamide compounds. US 9,714,234, 2017.

(32) Batt, D. G.; Bertrand, M. B.; Delucca, G.; Galella, M. A.; Ko, S. S.; Langevine, C. M.; Liu, Q.; Shi, Q.; Srivastava, A. S.; Tino, J. A.; Watterson, S. H. Substituted tetrahydrocarbazole and carbazole carboxamide compounds. US 9,334,290, 2016.

(33) Miyaura, N.; Suzuki, A. Palladium-catalyzed cross-coupling reactions of organoboron compounds. *Chem. Rev.* **1995**, *95*, 2457–2483.

■ NOTE ADDED AFTER ASAP PUBLICATION

This paper was originally published ASAP on September 22, 2020, with an error in the TOC/Abstract graphic. The corrected version was reposted on September 23, 2020.